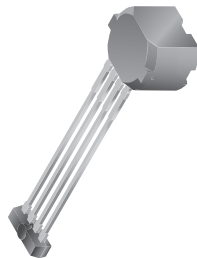


Dynamic, Self-Calibrating, Peak-Detecting, Differential Hall-Effect Gear Tooth Sensor IC

FEATURES AND BENEFITS

- Self-calibrating for tight timing accuracy
- First-tooth detection
- Immunity to air gap variation and system offsets
- Immunity to signature tooth offsets
- Integrated capacitor provides analog peak and valley information
- Low timing-accuracy drift with temperature changes
- Low radiated emissions
- Integrated, series resistor on VCC pin for improved transient immunity
- Large air gap capability
- Small, integrated package
- Optimized magnetic circuit
- Undervoltage lockout (UVLO)
- Wide operating voltage range

PACKAGE: 4-pin SIP (suffix SG)



Not to scale

DESCRIPTION

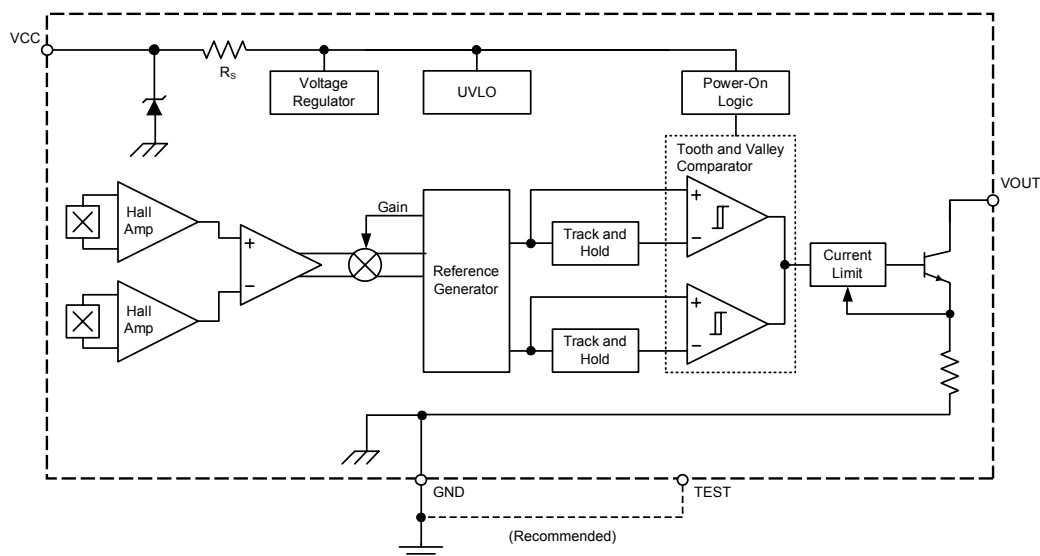
The ATS617 gear tooth sensor IC is a peak-detecting device that uses automatic gain control and an integrated capacitor to provide extremely accurate gear edge detection down to low operating speeds. Each device consists of a high-temperature plastic shell that holds together a samarium-cobalt pellet, a pole piece, and a differential open-collector Hall IC that has been optimized to the magnetic circuit. This small package can be easily assembled and used in conjunction with a wide variety of gear shapes and sizes.

The technology used for this device is Hall-effect based. The device incorporates a dual-element Hall IC that switches in response to differential magnetic signals created by ferromagnetic targets. The sophisticated processing circuitry contains an A-to-D converter that self-calibrates (normalizes) the internal gain of the device to minimize the effect of air gap variations. The patented peak-detecting filter circuit provides immunity to magnet and system offsets and has the ability to discriminate relatively fast changes such as those caused by tilt, gear wobble, and eccentricities. This easy-to-integrate solution provides first falling edge detection and stable operation to extremely low rpm. The ATS617 can be used as a replacement for the ATS616.

The ATS617 is ideal for use in systems that gather speed, position, and timing information using gear-tooth-based configurations. This device is particularly suited to those applications that

Continued on the next page...

Functional Block Diagram



ATS617LSG

Dynamic, Self-Calibrating, Peak-Detecting, Differential Hall-Effect Gear Tooth Sensor IC

DESCRIPTION (continued)

require extremely accurate duty cycle control or accurate edge-detection, such as automotive camshaft sensing.

The ATS617 is provided in a 4-pin SIP that is Pb (lead) free, with a 100% matte tin plated leadframe.

SELECTION GUIDE

Part Number	Packing*
ATS617LSGTN-T	13-in. reel, 800 pieces/reel

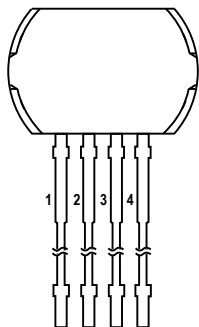
*Contact Allegro for additional packing options



ABSOLUTE MAXIMUM RATINGS

Characteristic	Symbol	Notes	Rating	Unit
Supply Voltage	V_{CC}	See Power Derating section	26.5	V
Reverse Supply Voltage	V_{RCC}		-18	V
Output Off Voltage	V_{OUTOFF}		24	V
Continuous Output Current	I_{OUT}		25	mA
Reverse Output Current	I_{ROUT}		50	mA
Operating Ambient Temperature	T_A	Range L	-40 to 150	°C
Maximum Junction Temperature	$T_J(max)$		165	°C
Storage Temperature	T_{stg}		-65 to 170	°C

Pinout Diagram



Terminal List

Number	Name	Function
1	VCC	Device supply
2	VOUT	Device output
3	Test	Tie to GND, or float
4	GND	Device ground

OPERATING CHARACTERISTICS: Over operating voltage and temperature range, unless otherwise noted

Characteristic	Symbol	Test Condition	Min.	Typ. [1]	Max.	Unit
ELECTRICAL CHARACTERISTICS						
Supply Voltage [2]	V_{CC}	Operating, $T_J < 165^\circ\text{C}$	4.5	–	24	V
Supply Protection Resistor	R_S		–	60	72	Ω
Undervoltage Lockout Threshold	$V_{CC(UV)}$	$V_{CC} = 0 \rightarrow 5\text{ V}; V_{CC} = 5 \rightarrow 0\text{ V}$	–	3.7	–	V
Output On Voltage	$V_{OUT(SAT)}$	$I_{OUT} = 15\text{ mA}$, output on	–	100	400	mV
Supply Zener Clamp Voltage	$V_{Zsupply}$	$I_{CC} = 15\text{ mA}$, $T_A = 25^\circ\text{C}$	28	–	–	V
Output Zener Clamp Voltage	$V_{Zoutput}$	$I_{OUT} = 3\text{ mA}$, $T_A = 25^\circ\text{C}$	30	–	–	V
Supply Zener Current	$I_{Zsupply}$	$V_S = 28\text{ V}$	–	–	15	mA
Output Zener Current	$I_{Zoutput}$	$V_{OUT} = 30\text{ V}$	–	–	3	mA
Output Current Limit	I_{OUTM}	$V_{OUT} = 12\text{ V}$	25	45	55	mA
Output Leakage Current	I_{OUTOFF}	$V_{OUT} = 24\text{ V}$, output off	–	–	15	μA
Supply Current	I_{CC}	$V_{CC} > V_{CC(min)}$	3	6	12	mA
Power-On Time	t_{PO}	$V_{CC} > 5\text{ V}$	–	80	500	μs
Power-On State	POS	$V_{CC} = 0 \rightarrow 5\text{ V}$	–	High	–	V
Output Rise Time [3]	t_r	$R_{PU} = 2\text{ k}\Omega$, $C_L = 4.7\text{ nF}$, 10% to 90%	–	21	–	μs
Output Fall Time	t_f	$V_{PU} = 5\text{ V}$, $R_{PU} = 2\text{ k}\Omega$, $C_L = 4.7\text{ nF}$, 90% to 10%	–	6	–	μs
		$V_{PU} = 12\text{ V}$, $R_{PU} = 2\text{ k}\Omega$, $C_L = 4.7\text{ nF}$, 90% to 10%	6	9	12	μs
PERFORMANCE CHARACTERISTICS						
Operating Air Gap Range	AG	Allegro reference target 60+2 operating at or above Minimum Operating Speed	0.4	–	2.5	mm
Operating Magnetic Flux Density Differential [4]	$B_{AG(p-p)}$	Operation at or above Minimum Operating Speed	60	–	–	G
Analog Signal Bandwidth	BW		–	15	–	kHz
Minimum Operating Speed	S_{OP}	Allegro 60+2 reference target	10	–	–	rpm

Continued on the next page...

OPERATING CHARACTERISTICS (continued) over operating voltage and temperature range, unless otherwise noted

Characteristic	Symbol	Test Condition	Min.	Typ. [1]	Max.	Unit
PERFORMANCE CHARACTERISTICS (continued)						
Initial Calibration Cycle [5]	n_{cal}	Output edges before calibration is completed, at $f_{sig} < 100$ Hz	–	1	–	edge
Calibration Mode Disable	n_{dis}	Output falling edges for startup calibration to be complete	64	64	64	edge
Relative Timing Accuracy, Sequential [6][7]	E_{θ}	Target Speed = 1000 rpm, $B_{AG(p-p)} > 100$ G	–	± 0.5	± 0.75	deg.
		Target Speed = 1000 rpm, $B_{AG(p-p)} > 60$ G	–	–	± 1.5	deg.
Allowable User Induced Differential Offset [4]	ΔB_{App}	Output switching only; may not meet data sheet specifications	–	–	± 50	G
Switching Hysteresis, Start-up	$V_{SWHYS(su)}$		–	190	–	mV
Switching Hysteresis, Running Mode	$V_{SWHYS(rm)}$		–	105	–	mV

[1] Typical data is at $V_{CC} = 12$ V and $T_A = 25^{\circ}\text{C}$. Performance may vary for individual units, within the specified maximum and minimum limits.

[2] Maximum voltage must be adjusted for power dissipation and junction temperature; see Power Derating section.

[3] This performance is not dominated by the design of the ATS617, it is determined primarily by the external interface circuitry.

[4] 1 G (gauss) = 0.1 mT (millitesla), exactly.

[5] Non-uniform magnetic profiles may require additional edges before calibration is complete.

[6] For Allegro 60+2 reference target.

[7] Accuracy may be compromised during the calibration cycle.

REFERENCE TARGET (GEAR) INFORMATION

REFERENCE TARGET 60+2

Characteristics	Symbol	Test Conditions	Typ.	Units	Symbol Key
Outside Diameter	D_o	Outside diameter of target	120	mm	
Face Width	F	Breadth of tooth, with respect to branded face	6	mm	
Angular Tooth Thickness	t	Length of tooth, with respect to branded face; measured at D_o	3	deg.	
Signature Region Angular Tooth Thickness	t_{SIG}	Length of signature tooth, with respect to branded face; measured at D_o	15	deg.	
Angular Valley Thickness	t_v	Length of valley, with respect to branded face; measured at D_o	3	deg.	
Tooth Whole Depth	h_t		3	mm	
Material		Low Carbon Steel	-	-	

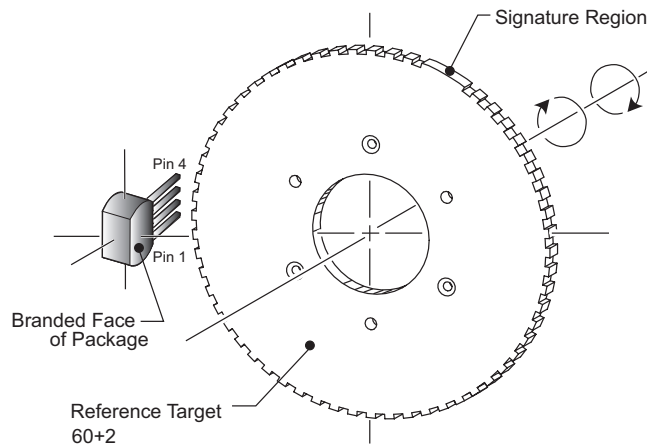
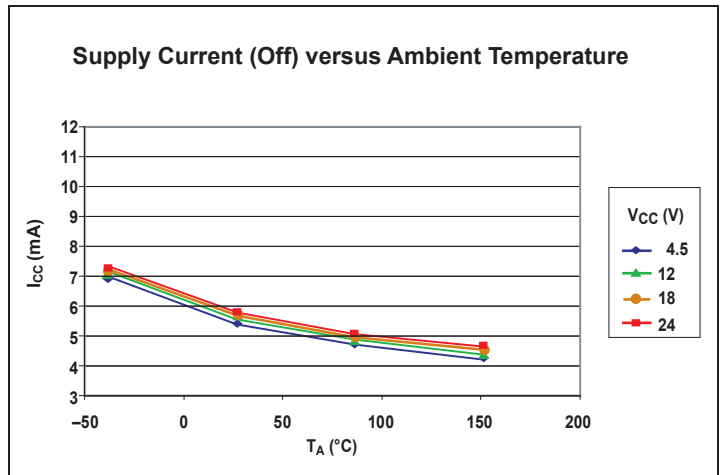
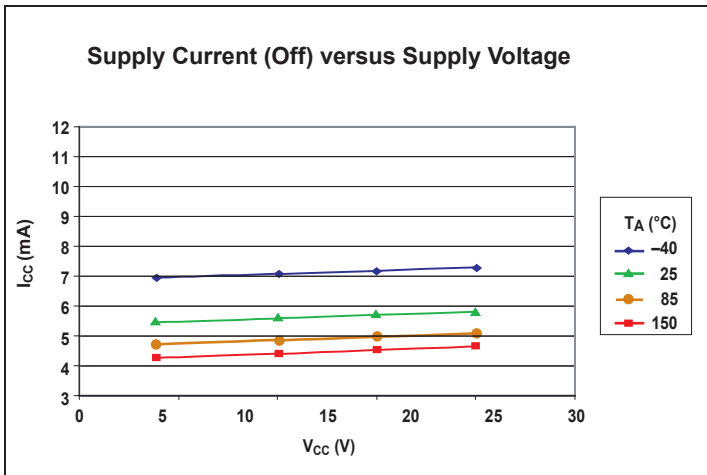
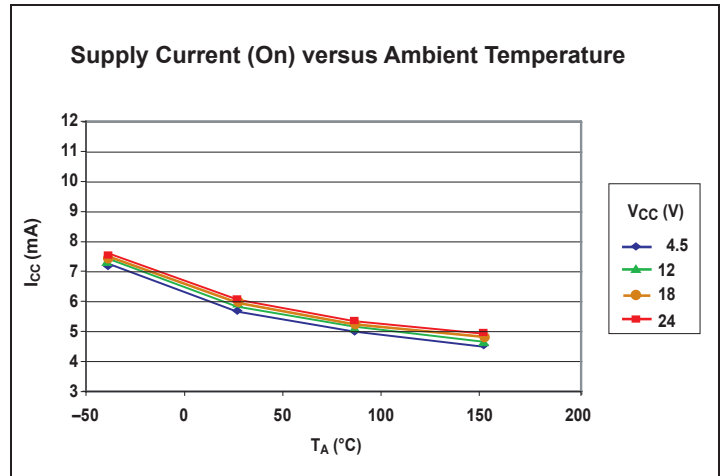
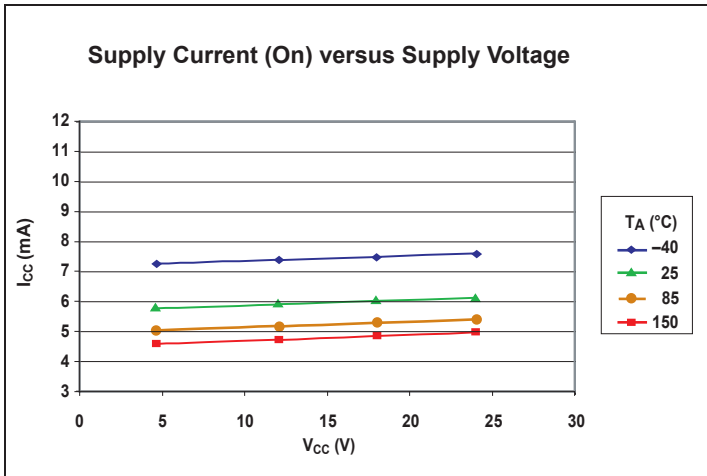
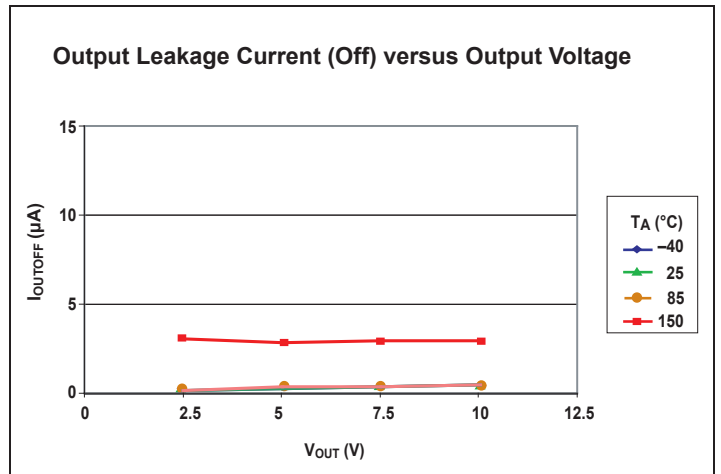
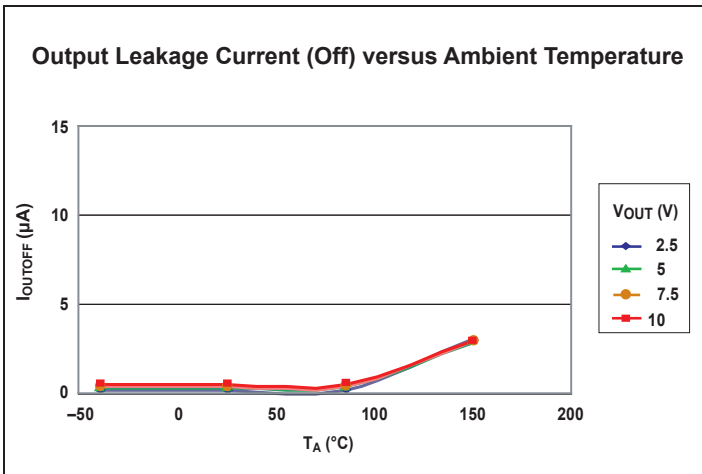
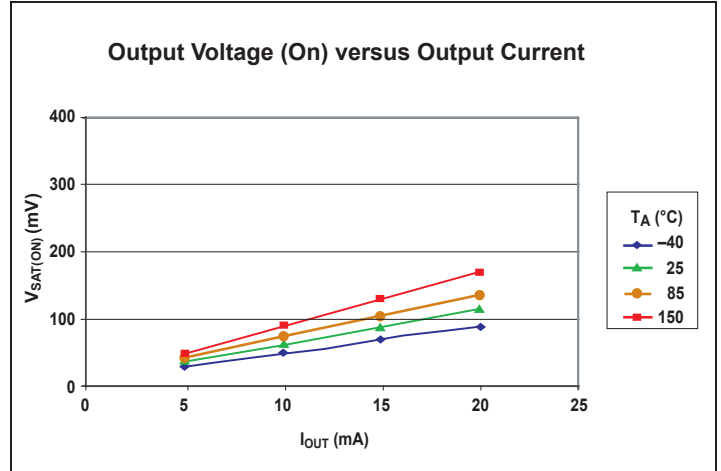
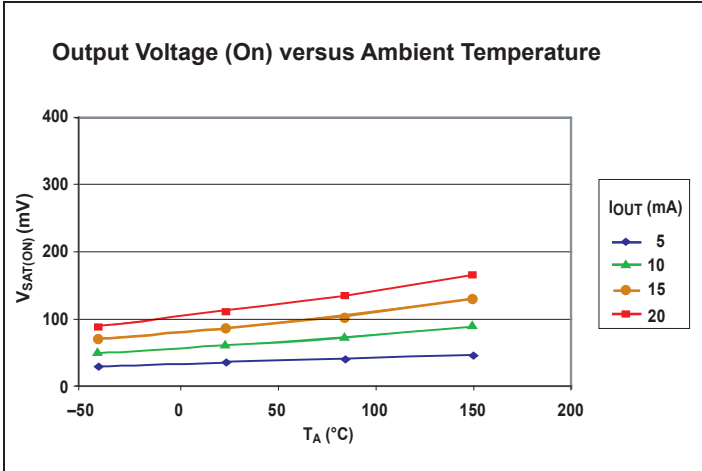


Figure 1. Configuration with Radial-Tooth Reference Target

CHARACTERISTIC DATA

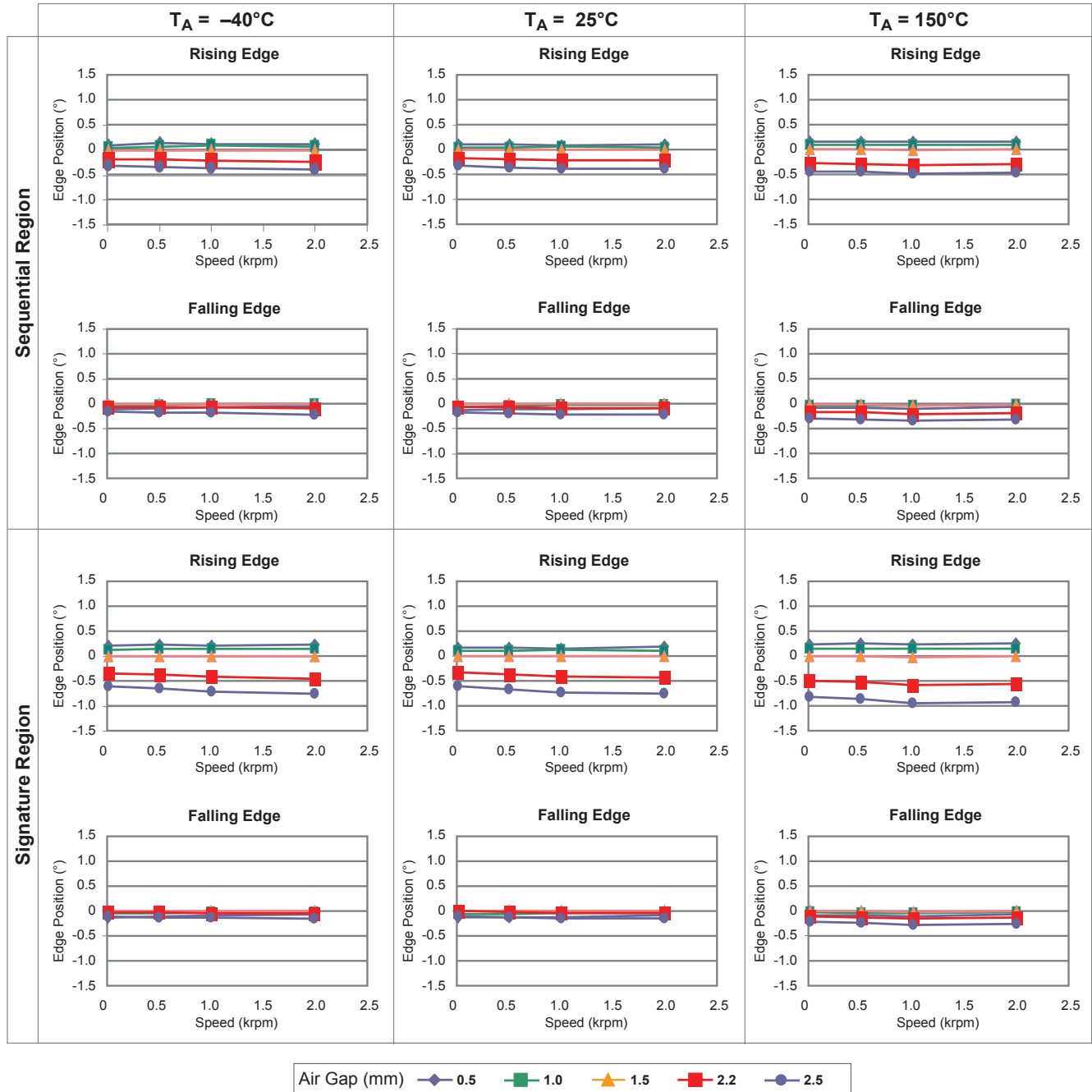


Continued on the next page.



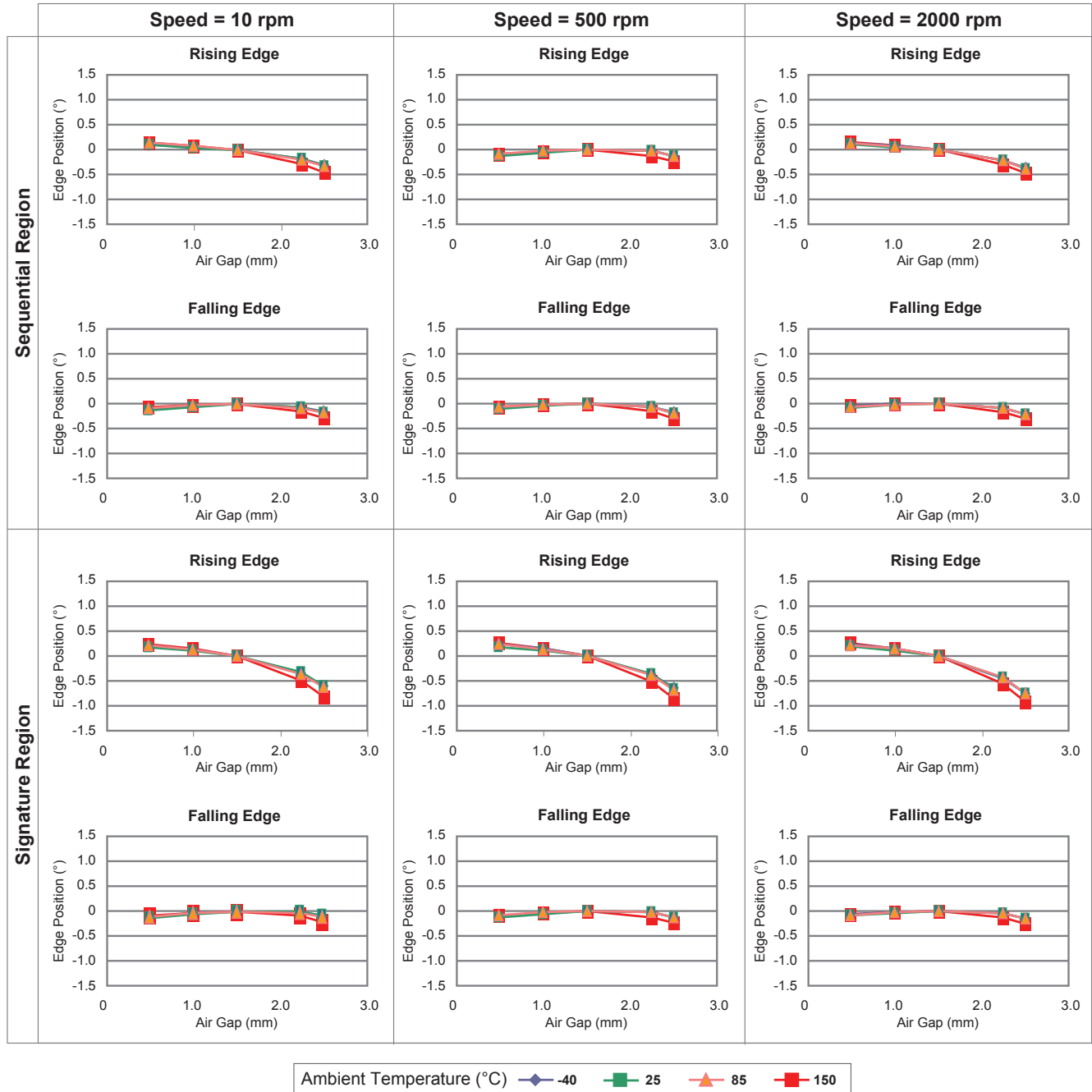
Continued on the next page.

Edge Position versus Target Speed through Ambient Temperature Range



Continued on the next page.

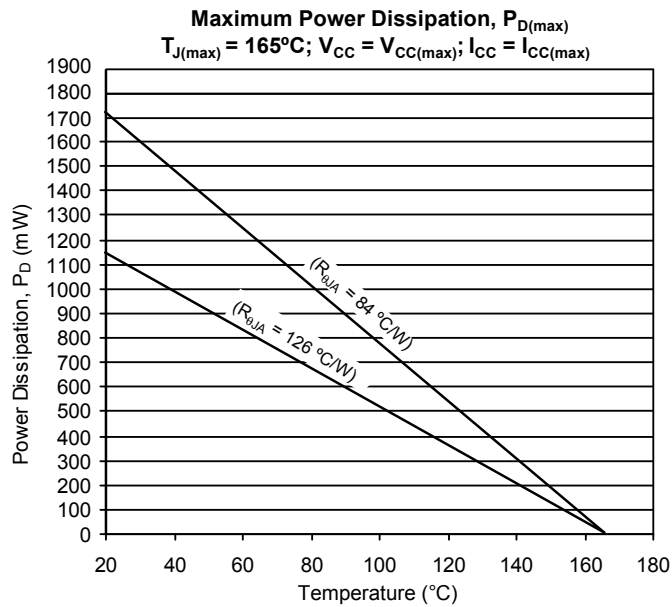
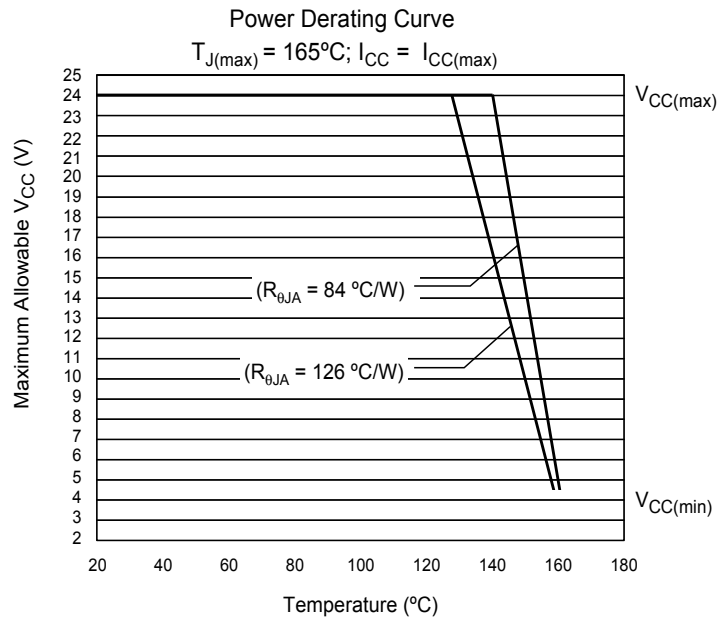
Edge Position versus Air Gap through Target Speed Range



THERMAL CHARACTERISTICS: May require derating at maximum conditions, see application information

Characteristic	Symbol	Test Conditions*	Value	Units
Package Thermal Resistance	$R_{\theta JA}$	Single-sided PCB with copper limited to solder pads	126	$^{\circ}\text{C}/\text{W}$
		Two-sided PCB with copper limited to solder pads and 3.57 in. ² (23.03 cm ²) of copper area each side, connected to GND pin	84	$^{\circ}\text{C}/\text{W}$

*Additional information is available on the Allegro website.



FUNCTIONAL DESCRIPTION

Assembly Description. The ATS617 gear tooth sensor IC is a Hall IC/rare-earth pellet configuration that is fully optimized to provide detection of gear tooth edges. This device is packaged in a molded miniature plastic body that has been optimized for size, ease of assembly, and manufacturability. High operating temperature materials are used in all aspects of construction.

After proper power is applied to the component, the chip is capable of instantly providing digital information that is representative of the profile of a rotating gear. No additional optimization or processing circuitry is required. This ease of use should reduce design time and incremental assembly costs for most applications.

Hall Technology. The ATS617 contains a single-chip differential Hall-effect sensor IC, a samarium cobalt pellet, and a flat ferrous pole piece (figure 2). The Hall IC consists of 2 Hall elements (spaced 2.2 mm apart) located so as to measure the magnetic gradient created by the passing of a ferrous object. The two elements measure the magnetic gradient and convert it to an analog voltage that is then processed in order to provide a digital output signal.

The Hall IC is self-calibrating and also possesses a temperature compensated amplifier and offset cancellation circuitry. Its voltage regulator provides supply noise rejection throughout the operating voltage range. Changes in temperature do not greatly affect this device due to the stable amplifier design and the offset

rejection circuitry. The Hall transducers and signal processing electronics are integrated on the same silicon substrate, using a proprietary BiCMOS process.

Internal Electronics. The processing circuit uses a patented peak detection scheme to eliminate magnet and system offsets. This technique allows dynamic coupling and filtering of offsets without the power-up and settling time disadvantages of classical high-pass filtering schemes. The peak signal of every tooth and valley is detected by the filter and is used to provide an instant reference for the operate and release point comparator. In this manner, the thresholds are adapted and referenced to individual signal peaks and valleys, providing immunity to zero line variation from installation inaccuracies (tilt, rotation, and off-center placement), as well as for variations caused by target and shaft eccentricities.

The ATS617 also includes self-calibration circuitry that is engaged at power on. The signal amplitude is measured, and then the device gain is normalized. In this manner switch point drift versus air gap is minimized, and excellent timing accuracy can be achieved.

The AGC (Automatic Gain Control) circuitry, in conjunction with a unique hysteresis circuit, also eliminates the effect of gear edge overshoot as well as increases the immunity to false switching caused by gear tooth anomalies at close air gaps. The AGC circuit sets the gain of the device after power-on.

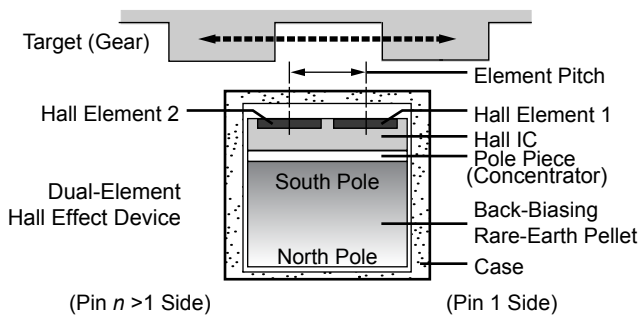


Figure 2. Relative motion of the target is detected by the dual Hall elements mounted on the Hall IC.

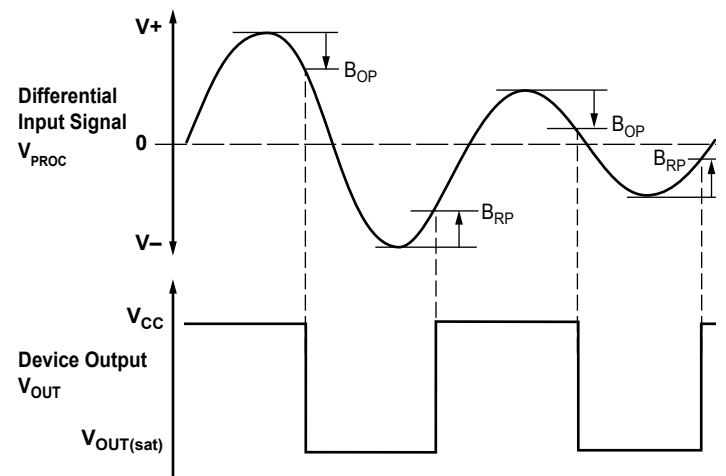


Figure 3. The peaks in the resulting differential signal are used to set the operate, B_{OP} , and release, B_{RP} , switch points.

Superior Performance. The ATS617 peak-detecting differential design has several advantages over conventional Hall-effect gear tooth sensors. The signal-processing techniques used in the ATS617 solve the catastrophic issues that affect the functionality of conventional digital gear tooth sensors, such as the following:

- *Temperature drift.* Changes in temperature do not greatly affect this device due to the stable amplifier design and the offset rejection circuitry.
- *Timing accuracy variation due to air gap.* The accuracy variation caused by air gap changes is minimized by the self-calibration circuitry. A 2×-to-3× improvement can be seen.
- *Dual edge detection.* Because this device switches based on the positive and negative peaks of the signal, dual edge detection is guaranteed.
- *Tilted or off-center installation.* Traditional differential sensors can switch incorrectly due to baseline changes versus air gap caused by tilted or off-center installation. The peak detector circuitry references the switch point from the peak and is immune to this failure mode. There may be a timing accuracy shift caused by this condition.
- *Large operating air gaps.* Large operating air gaps are achievable with this device due to the sensitive switch points after power-on (dependent on target dimensions, material, and speed).

- *Immunity to magnetic overshoot.* The patented adjustable hysteresis circuit makes the ATS617 immune to switching on magnetic overshoot within the specified air gap range.
- *Response to surface defects in the target.* The gain-adjust circuitry reduces the effect of minor gear anomalies that would normally cause false switching.
- *Immunity to vibration and backlash.* The gain-adjust circuitry keeps the hysteresis of the device roughly proportional to the peak-to-peak signal. This allows the device to have good immunity to vibration even when operating at close air gaps.
- *Immunity to gear run out.* The differential chip configuration eliminates the baseline variations caused by gear run out

Differential vs. Single-Element Design. The differential chip is superior in most applications to the classical single-element design. The single-element configuration commonly used (Hall-effect element mounted on the face of a simple permanent magnet) requires the detection of a small signal (often <100 G) that is superimposed on a large back-biased field, often 1500 G to 3500 G. For most gear/target configurations, the back-biased field values change due to concentration effects, resulting in a varying baseline with air gap, valley widths, eccentricities, and vibration (figure 4). The differential configuration (figure 5) cancels the effects of the back-biased field and avoids many of the issues presented by the single Hall element design.

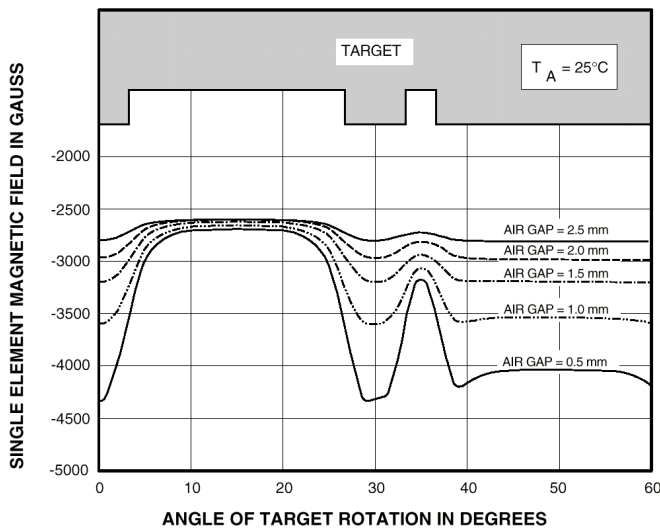


Figure 4. Effect of varying valley widths on single-element circuits.

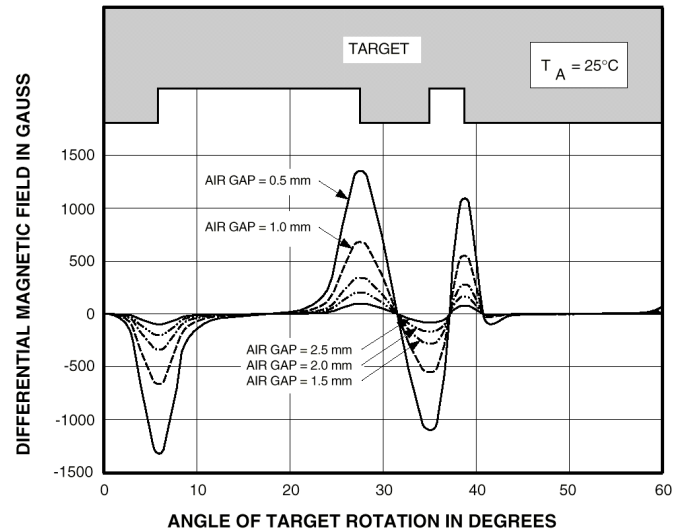


Figure 5. Effect of varying air gaps on differential circuits.

Peak Detecting vs. AC-Coupled Filters. High-pass filtering (normal AC coupling) is a commonly used technique for eliminating circuit offsets. However, AC coupling has errors at power-on because the filter circuit needs to hold the circuit zero value even though the circuit may power-on over a large signal. Such filtering techniques can only perform properly after the filter has been allowed to settle, which typically takes longer than 1s. Also, high-pass filter solutions cannot easily track rapidly changing baselines, such as those caused by eccentricities. (The term *baseline* refers to a 0 G differential field, where each Hall-effect element is subject to the same magnetic field strength; see figure 3.) In contrast, peak detecting designs switch at the change in slope of the differential signal, and so are baseline-independent both at power-on and while running.

Peak Detecting vs. Zero-Crossing Reference. The usual differential zero-crossing sensor ICs are susceptible to false switching due to off-center and tilted installations that result in a shift of the baseline that changes with air gap. The track-and-hold peak detection technique ignores baseline shifts versus air gaps and provides increased immunity to false switching. In addition, using track-and-hold peak detection techniques, increased air gap capabilities can be expected because peak detection utilizes the entire peak-to-peak signal range, as compared to zero-crossing detectors, which switch at half the peak-to-peak signal.

Power-On Operation. The device powers-on in the Off state (output voltage high), irrespective of the magnetic field condition. The circuit is then ready to accurately detect the first target edge that results in a high-to-low transition of the device output.

Undervoltage Lockout (UVLO). When the supply voltage, V_{CC} , is below the minimum operating voltage, $V_{CC(UV)}$, the device is off and stays off, irrespective of the state of the magnetic field. This prevents false signals, which may be caused by undervoltage conditions (especially during power-up), from appearing at the output.

Output. The device output is an open-drain stage. An external pull-up (resistor) must be supplied to a supply voltage of not more than $V_{CC(max)}$.

Output Polarity. The output of the unit will switch from low to high as the leading edge of a tooth passes the branded face of the package in the direction indicated in figure 6. This means that in such a configuration, the output voltage will be high when the package is facing a tooth. If the target rotation is in the opposite direction relative to the package, the output polarity will be opposite as well, with the unit switching from low to high as the leading edge passes the unit.

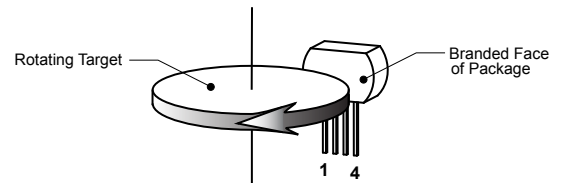


Figure 6. This left-to-right (pin 1 to pin 4) direction of target rotation results in a high output signal when a tooth of the target gear is nearest the branded face of the package. A right-to-left (pin 4 to pin 1) rotation inverts the output signal polarity.

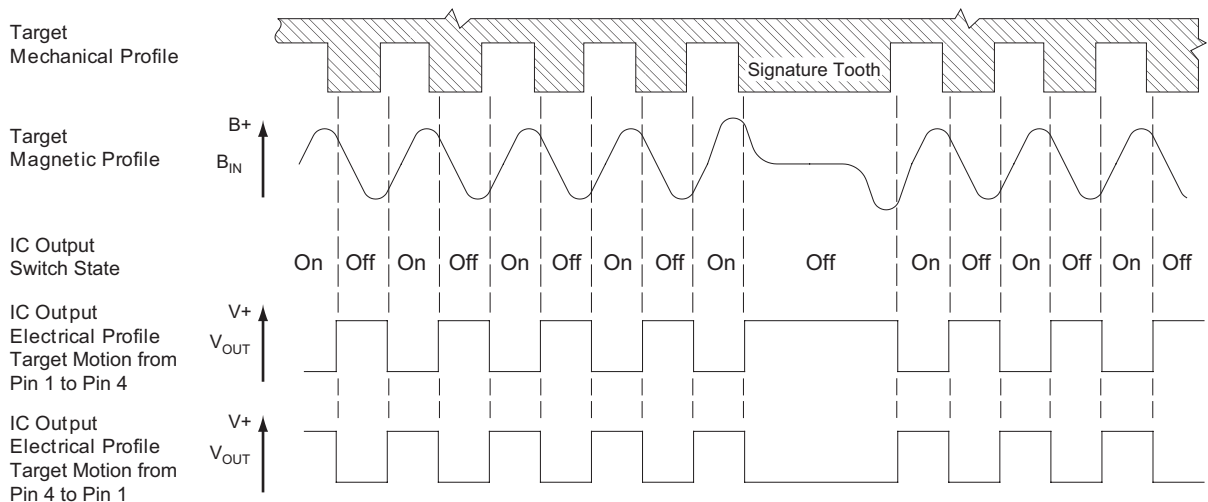


Figure 7. The magnetic profile reflects the geometry of the target, allowing the device to present an accurate digital output response.

POWER DERATING

The device must be operated below the maximum junction temperature of the device, $T_{J(max)}$. Under certain combinations of peak conditions, reliable operation may require derating supplied power or improving the heat dissipation properties of the application. This section presents a procedure for correlating factors affecting operating T_J . (Thermal data is also available on the Allegro MicroSystems website.)

The Package Thermal Resistance, $R_{\theta JA}$, is a figure of merit summarizing the ability of the application and the device to dissipate heat from the junction (die), through all paths to the ambient air. Its primary component is the Effective Thermal Conductivity, K , of the printed circuit board, including adjacent devices and traces. Radiation from the die through the device case, $R_{\theta JC}$, is relatively small component of $R_{\theta JA}$. Ambient air temperature, T_A , and air motion are significant external factors, damped by overmolding.

The effect of varying power levels (Power Dissipation, P_D), can be estimated. The following formulas represent the fundamental relationships used to estimate T_J , at P_D .

$$P_D = V_{IN} \times I_{IN} \quad (1)$$

$$\Delta T = P_D \times R_{\theta JA} \quad (2)$$

$$T_J = T_A + \Delta T \quad (3)$$

For example, given common conditions such as: $T_A = 25^\circ\text{C}$, $V_{CC} = 12\text{ V}$, $I_{CC} = 6\text{ mA}$, and $R_{\theta JA} = 126\text{ }^\circ\text{C/W}$, then:

$$P_D = V_{CC} \times I_{CC} = 12\text{ V} \times 6\text{ mA} = 72\text{ mW}$$

$$\Delta T = P_D \times R_{\theta JA} = 72\text{ mW} \times 126\text{ }^\circ\text{C/W} = 9^\circ\text{C}$$

$$T_J = T_A + \Delta T = 25^\circ\text{C} + 9^\circ\text{C} = 34^\circ\text{C}$$

A worst-case estimate, $P_D(max)$, represents the maximum allowable power level ($V_{CC}(max)$, $I_{CC}(max)$), without exceeding $T_J(max)$, at a selected $R_{\theta JA}$ and T_A .

Example: Reliability for V_{CC} at $T_A = 150^\circ\text{C}$, package SG, using minimum-K PCB.

Observe the worst-case ratings for the device, specifically: $R_{\theta JA} = 126\text{ }^\circ\text{C/W}$, $T_J(max) = 165^\circ\text{C}$, $V_{CC}(max) = 24\text{ V}$, and $I_{CC}(max) = 12\text{ mA}$.

Calculate the maximum allowable power level, $P_D(max)$. First, invert equation 3:

$$\Delta T_{max} = T_J(max) - T_A = 165^\circ\text{C} - 150^\circ\text{C} = 15^\circ\text{C}$$

This provides the allowable increase to T_J resulting from internal power dissipation. Then, invert equation 2:

$$P_D(max) = \Delta T_{max} \div R_{\theta JA} = 15^\circ\text{C} \div 126\text{ }^\circ\text{C/W} = 119\text{ mW}$$

Finally, invert equation 1 with respect to voltage:

$$V_{CC}(est) = P_D(max) \div I_{CC}(max) = 119\text{ mW} \div 12\text{ mA} = 9.92\text{ V}$$

The result indicates that, at T_A , the application and device can dissipate adequate amounts of heat at voltages $\leq V_{CC}(est)$.

Compare $V_{CC}(est)$ to $V_{CC}(max)$. If $V_{CC}(est) \leq V_{CC}(max)$, then reliable operation between $V_{CC}(est)$ and $V_{CC}(max)$ requires enhanced $R_{\theta JA}$. If $V_{CC}(est) \geq V_{CC}(max)$, then operation between $V_{CC}(est)$ and $V_{CC}(max)$ is reliable under these conditions.

This value applies only to the voltage drop across the ATS617 chip. If a protective series diode or resistor is used, the effective maximum supply voltage is increased. For example, when a standard diode with a 0.7 V drop is used:

$$V_{CC}(max) = 9.9\text{ V} + 0.7\text{ V} = 10.6\text{ V}$$

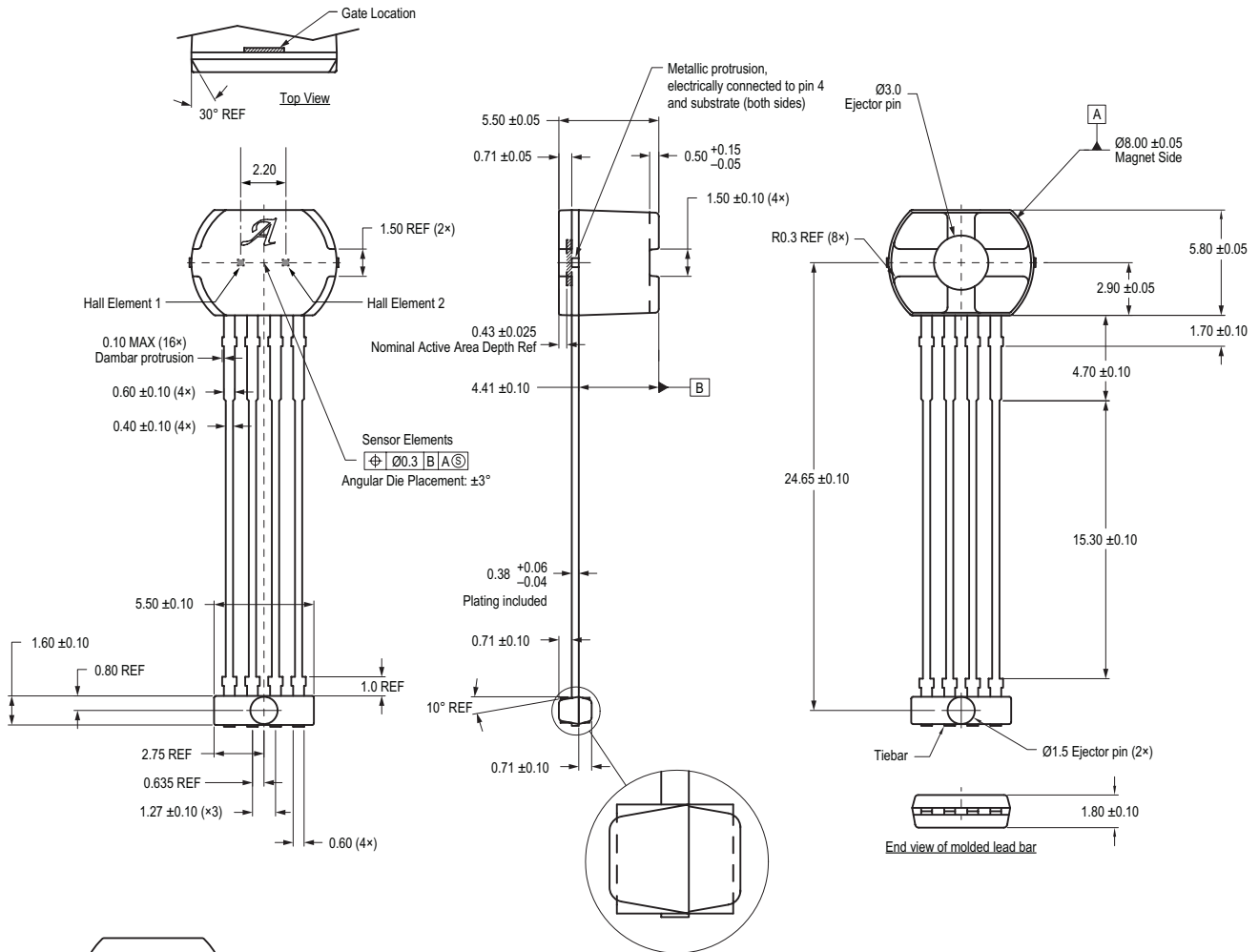
Package SG 4-Pin SIP

For Reference Only – Not for Tooling Use

(Reference DWG-0000392)

Dimensions in millimeters. NOT TO SCALE.

Dimensions exclusive of mold flash, gate burrs, and dambar protrusions
Exact case and lead configuration at supplier discretion within limits shown



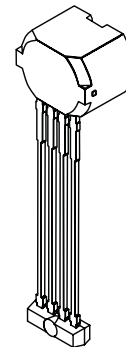
Standard Branding Reference View

Lines 2, 3, 4 = 7 characters.

- Line 1: Logo A molded in
- Line 2: 7-digit alpha numeric Lot Number
- Line 3: Last 3 digit of Part Number.
Additional suffixes may be added to Part number as required.
- Line 4: 4-digit Date Code

Center align

Branding scale and appearance at supplier discretion



Revision History

Number	Date	Description
2	May 20, 2020	Minor editorial updates
3	June 15, 2021	Updated Package Outline Drawing (page 15)

The products described herein are manufactured under one or more of the following U.S. patents: 5,264,783; 5,389,889; 5,442,283; 5,517,112; 5,581,179; 5,619,137; 5,621,319; 5,650,719; 5,686,894; 5,694,038; 5,729,130; 5,917,320; 6,091,239; 6,100,680; 6,232,768; 6,242,908; 6,265,865; 6,297,627; 6,525,531; 6,690,155; 6,693,419; 6,919,720; 7,046,000; 7,053,674; 7,138,793; 7,199,579; 7,253,614; 7,365,530; 7,368,904; or other patents pending.

Copyright 2021, Allegro MicroSystems.

Allegro MicroSystems reserves the right to make, from time to time, such departures from the detail specifications as may be required to permit improvements in the performance, reliability, or manufacturability of its products. Before placing an order, the user is cautioned to verify that the information being relied upon is current.

Allegro's products are not to be used in any devices or systems, including but not limited to life support devices or systems, in which a failure of Allegro's product can reasonably be expected to cause bodily harm.

The information included herein is believed to be accurate and reliable. However, Allegro MicroSystems assumes no responsibility for its use; nor for any infringement of patents or other rights of third parties which may result from its use.

Copies of this document are considered uncontrolled documents.

For the latest version of this document, visit our website:

www.allegromicro.com